



OPEN Evaluation of Bridge Capture technology for mutation profiling in liquid biopsies of metastatic colorectal cancer patients

Aparna Ganesan^{1,2,14}✉, Anttoni Korhikoski^{3,4,14}, Simona Adamusová^{3,4,14}, Anna Musku³, Tuula Rantasalo³, Nea Laine³, Emma Andersson⁵, Emerik Osterlund^{6,7}, Ali Ovissi⁸, Päivi Halonen⁹, Tatu Hirvonen³, Jorma Kim³, Jukka Laine^{3,4,10}, Antti Silvonieminen^{10,11}, Heikki Minn¹⁰, Juuso Blomster^{3,4}, Anna-Kaisa Anttonen⁵, Soili Kytölä⁵, Pia Osterlund^{9,12,13}, Juha-Pekka Pursiheimo³, Pirjo Nummela^{1,2}, Manu Tamminen^{3,4,15} & Ari Ristimäki^{1,2,15}

Colorectal cancer (CRC) is the second leading cause of cancer-related deaths, often presenting at an advanced stage with significant molecular heterogeneity. This is the first study to evaluate the performance of a novel next-generation sequencing (NGS)-based Bridge Capture technology for mutation profiling and minimal residual disease detection in circulating tumor (ct)DNA from metastatic colorectal cancer (mCRC) patients. Its performance was compared to those of droplet digital PCR (ddPCR), Ion AmpliSeq Cancer Hotspot Panel v2, and Idylla ctKRAS Mutation Assay. Eighty serial plasma samples from ten mCRC patients were analyzed by Bridge Capture and ddPCR, demonstrating a very strong correlation in variant allele frequency (VAF) values ($r_s = 0.86$). The concordance of Bridge Capture with ddPCR ($\kappa = 0.70$) and Idylla ($\kappa = 0.79$) showed substantial agreement. A subset of samples ($n = 10$) was analyzed using the Ion AmpliSeq NGS-panel and both methods identified 15 driver mutations with strong correlation of VAF values ($r_s = 0.74$). Additionally, Bridge Capture identified several oncogenic mutations beyond those detected by Ion AmpliSeq, highlighting its comprehensive profiling capability. The scalability of Bridge Capture was validated using an expanded panel and synthetic DNA targets, showing a strong linear correlation between observed and expected VAF values. This study demonstrates the scalability and accuracy of the Bridge Capture platform, and its potential to enhance mutation detection and clinical decision-making using ctDNA samples from patients with mCRC.

Keywords Bridge Capture, Colorectal cancer, cfDNA, ctDNA, ddPCR, NGS

¹Applied Tumor Genomics Research Program, Research Programs Unit, University of Helsinki, Helsinki, Finland. ²Department of Pathology, HUS Diagnostic Center, Helsinki University Hospital and University of Helsinki, Helsinki, Finland. ³Genomill Health Inc, Turku, Finland. ⁴Department of Biology, University of Turku, Turku, Finland. ⁵Department of Genetics, HUS Diagnostic Center, Helsinki University Hospital and University of Helsinki, Helsinki, Finland. ⁶Department of Surgery, Helsinki University Hospital and University of Helsinki, Helsinki, Finland. ⁷Department of Immunology, Genetics and Pathology, Uppsala University, Uppsala, Sweden. ⁸Department of Radiology, HUS Diagnostic Center, Helsinki University Hospital and University of Helsinki, Helsinki, Finland. ⁹Department of Oncology, Comprehensive Cancer Center, Helsinki University Hospital and University of Helsinki, Helsinki, Finland. ¹⁰Department of Oncology, Turku University Hospital, Turku, Finland. ¹¹Department of Otorhinolaryngology – Head and Neck Surgery, Turku University Hospital and University of Turku, Turku, Finland. ¹²Department of Oncology, Tampere University Hospital and University of Tampere, Tampere, Finland. ¹³Department of Oncology/Pathology, Karolinska University Hospital and Karolinska Institute, Stockholm, Sweden. ¹⁴These authors contributed equally: Aparna Ganesan, Anttoni Korhikoski and Simona Adamusová. ¹⁵These authors jointly supervised this work: Manu Tamminen and Ari Ristimäki. ✉email: aparna.ganesan@helsinki.fi; manu@genomill.com

Abbreviations

cfDNA	Cell-free DNA
CHPv2	Cancer Hotspot Panel version 2
CI	Confidence interval
CRC	Colorectal cancer
ctDNA	Circulating tumor DNA
ddPCR	Droplet digital PCR
IQR	Interquartile range
mCRC	Metastatic colorectal cancer
MRD	Minimal residual disease
NGS	Next-generation sequencing
r	Pearson correlation coefficient
r_s	Spearman correlation coefficient
R^2	Coefficient of determination
UMI	Unique molecular identifier
VAF	Variant allele frequency

Colorectal cancer (CRC) is the third most common cancer and the second leading cause of cancer deaths¹. CRC presents as a metastatic disease in 15–30% of the cases. Moreover, 20–50% of those initially diagnosed with localized disease develop metastases during the follow up². At the molecular level, CRC is a heterogeneous disease, with various subtypes exhibiting distinct genetic characteristics that guide treatment strategies^{3,4}. For example, mutations in the *KRAS* gene are predictive indicators of resistance to therapies targeting the epidermal growth factor receptor (EGFR) in cases of metastatic colorectal cancer (mCRC)^{4,5}.

Liquid biopsy is a minimally invasive alternative to traditional tissue biopsy and imaging modalities for cancer diagnostics. The most common type of liquid biopsy is plasma-derived cell-free (cf.)DNA, which contains a small fraction of circulating tumor (ct)DNA. Analyzing mutations in ctDNA can facilitate monitoring of treatment responses, detection of minimal residual disease (MRD), and identification of resistance-associated mutations^{6,7}.

Mutations in liquid biopsies can be detected using several methods. Droplet digital PCR (ddPCR) is a highly sensitive and specific technique that enables the quantification of target mutations, making it particularly useful for detecting low-frequency mutations^{8,9}. However, the main limitations of ddPCR include the need for prior knowledge of the tumor mutation profile and the restricted number of mutations that can be analyzed in a single reaction. Another recently introduced targeted platform, Idylla, offers a fully automated, real-time PCR-based technology with a fast turnaround time. It enables the analysis of ctDNA mutations directly from plasma samples without requiring a separate cfDNA extraction^{10,11}. While Idylla is particularly suited for timely clinical decision-making, it does not provide variant allele frequency (VAF) or the exact identity of the mutation.

Next-generation sequencing (NGS) is one of the most promising methods for comprehensive ctDNA analysis. It allows for the simultaneous analysis of a large panel of DNA variants, providing broader and more detailed insights into the mutation profile. This is particularly valuable in cases of tumor relapse, enabling the identification of resistance mutations, which could potentially lead to better treatment outcomes^{12,13}. Additionally, the extensive coverage of NGS panels enables ctDNA analysis, such as MRD detection, without requiring prior knowledge of mutations present in the tumor tissue. However, NGS-based technologies have certain limitations, including lower sensitivity compared to ddPCR, the need for specialized expertise in data analysis, and higher costs.

Bridge Capture is a novel NGS-based technology utilizing a proprietary probe design consisting of two target-specific probes connected by a bridge oligonucleotide, ensuring simultaneous hybridization to adjacent sequences on the target molecule¹⁴. This probe configuration enhances specificity, minimizes off-target binding, and improves the accuracy of target enrichment, making Bridge Capture an attractive platform for detecting low-frequency variants. It also incorporates unique molecular identifiers (UMIs) into predefined regions of the probes, enabling accurate target quantification via effective error correction. Bridge Capture technology is also highly scalable, allowing for the expansion of panel content.

In this study, we demonstrate, for the first time, the performance of the novel NGS-based Bridge Capture technology in clinical ctDNA samples. We compared it to ddPCR, the NGS-based Ion AmpliSeq Cancer Hotspot Panel v2 (CHPv2), and the Idylla ctKRAS Mutation Assay for mutation profiling and MRD screening in ctDNA samples. The analysis was conducted on eighty serial plasma samples from ten mCRC patients. Additionally, the scalability of Bridge Capture was evaluated using an expanded panel and synthetic DNA.

Results

Comparison of Bridge Capture and ddPCR in detecting *KRAS* mutations in ctDNA samples

Design of the study involving eighty serial plasma samples from ten mCRC patients is shown in Fig. 1a. Each patient had an oncogenic *KRAS* mutation identified in their primary tumor tissue specimen, enabling a tumor-informed approach to ctDNA analysis. The Bridge Capture 282-probe panel and ddPCR detected *KRAS* mutations in 35 of the 80 ctDNA samples (44%), while 33 samples (41%) were negative with both methods (Table 1). Eight ctDNA samples (10%) were positive with the Bridge Capture method but negative with ddPCR, while four samples (5%) were positive with ddPCR but negative with Bridge Capture. The concordance between these two technologies was 0.70 (95% confidence interval [CI]: 0.55–0.86) using kappa statistics, indicating a substantial level of agreement between the two methods. Notably, the disagreements between the methods were observed mainly at relatively low VAF values (Bridge Capture median 0.03%; range 0–7.74%; Table 2). Further, the samples that were positive by ddPCR but negative by Bridge Capture had a median cfDNA input of 4 ng

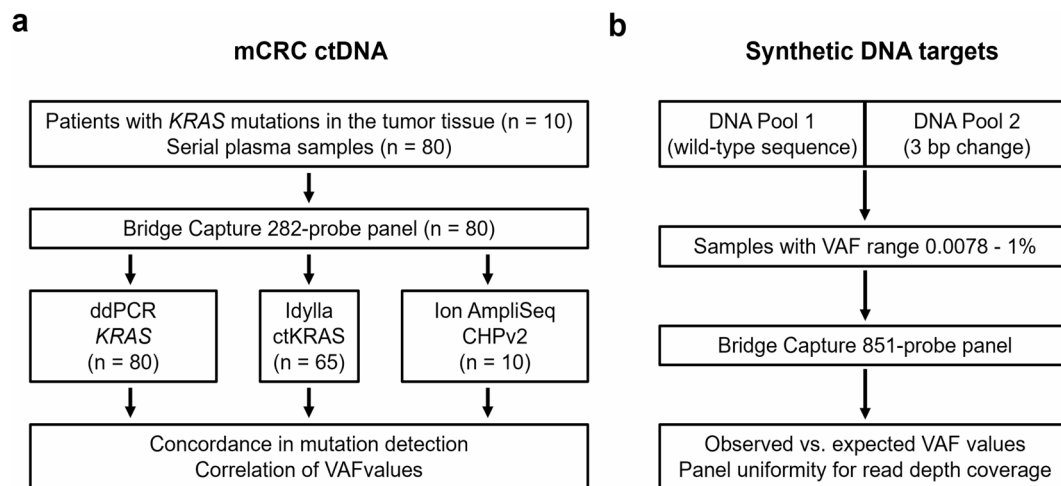


Fig. 1. Design of the study. Evaluation of Bridge Capture technology using (a) circulating tumor (ct)DNA extracted from plasma samples of metastatic colorectal cancer (mCRC) patients and (b) synthetic DNA targets. Fifteen plasma samples were not analyzable with Idylla due to lack of *KRAS* G13R mutation in the assay cassette (12 samples) or lack of enough plasma sample (three samples). Initially, the last sample of each patient was analyzed in comparison with Ion AmpliSeq, and subsequently all discrepant samples as analyzed using Bridge Capture versus ddPCR ($n = 12$) were also analyzed by Ion AmpliSeq. ddPCR: droplet digital PCR; CHPv2: Cancer Hotspot Panel version 2; VAF: variant allele frequency.

		Bridge Capture	
		Positive	Negative (VAF 0%)
ddPCR	Positive	35	4
	Negative	8	33

Table 1. Concordance between Bridge Capture and ddPCR in detecting *KRAS* mutations in ctDNA samples ($n = 80$). Cohen's Kappa-value was 0.70.

Patient number	Sampling time (months)	<i>KRAS</i> variant	Amino acid change	Bridge Capture VAF (%)	ddPCR VAF (%)	Ion AmpliSeq CHPv2 VAF (%)	Idylla assay
2	9	c.37G>C	p.G13R	0.03	Negative	0.00	Not included*
	19	c.37G>C	p.G13R	3.49	Negative	0.00	Not included*
4	2	c.35G>T	p.G12V	0.03	Negative	0.00	Negative
	5	c.35G>T	p.G12V	0.03	Negative	0.00	Positive
5	12	c.34G>T	p.G12C	2.42	Negative	0.00	Positive
6	19	c.35G>A	p.G12D	0.02	Negative	0.00	Not available**
8	1	c.35G>A	p.G12D	0.03	Negative	0.00	Negative
	18	c.35G>A	p.G12D	7.74	Negative	1.53	Positive
1	10	c.35G>A	p.G12D	0.00	1.80	2.15	Positive
5	0	c.34G>T	p.G12C	0.00	0.20	0.00	Positive
6	0	c.35G>A	p.G12D	0.00	5.20	0.55	Positive
	1	c.35G>A	p.G12D	0.00	0.30	0.00	Invalid***

Table 2. Bridge Capture and ddPCR discrepant samples analyzed using Ion AmpliSeq CHPv2 and Idylla ct*KRAS* mutation assay. **KRAS* p.G13R is not included in the Idylla cartridge. **The sample was not available for Idylla analysis. ***Idylla analysis was invalid.

(range 3–5 ng) and those positive by Bridge Capture but negative by ddPCR 14 ng (range 9–54 ng), whereas those that were positive by both methods had a median ctDNA input of 40 ng (range 5–795 ng; Supplementary Table S1).

A very strong correlation in VAF values was observed between Bridge Capture and ddPCR across all samples ($n=80$), with a Spearman correlation coefficient (r_s) of 0.86 (95% CI: 0.78–0.91; $P<0.0001$) (Fig. 2a). In the subset of samples with low VAF values ($\leq 10\%$), excluding discrepant cases and those that tested negative by both methods, the r_s was 0.50 (95% CI: 0.02–0.79; $P=0.04$; $n=18$), indicating a moderate correlation (Supplementary Fig. S1). *KRAS* VAF values for all plasma samples of eight mCRC patients are shown in Fig. 3, as analyzed by Bridge Capture and ddPCR. For the other two patients, all ctDNA samples were negative with both methods. These patients had only peritoneal metastases as detected by radiology. As we and others have previously shown, CRC patients with peritoneal metastases have very low levels of ctDNA^{15,16}.

Comparison of Bridge Capture and Idylla ct*KRAS* mutation assay in detecting *KRAS* mutations in ctDNA samples

Of the 80 plasma samples, 65 were analyzed using the Idylla ct*KRAS* Mutation Assay (Supplementary Table S1). Fifteen samples were left out due to the lack of *KRAS* G13R mutation in the assay cassette (12 samples) or lack of enough plasma sample (three samples). Out of 65 samples, 58 were analyzed successfully, whereas five samples gave an error (cassette error), and two samples gave invalid results. Among the successful cases, 31 samples (54%) were concordantly positive, and 21 samples (36%) concordantly negative (Table 3). Two samples (3%) were positive by Bridge Capture and negative by Idylla, while four samples (7%) were negative by Bridge Capture and positive by Idylla. The concordance between these two technologies was 0.79 (95% CI: 0.63–0.95), using kappa statistics, indicating a substantial level of agreement between the two methods.

Comparison of Bridge Capture and Ion AmpliSeq in detecting CRC driver mutations in ctDNA samples

The last serial plasma sample of each mCRC patient ($n=10$) was analyzed using the Ion AmpliSeq CHPv2 NGS panel. Both Bridge Capture and Ion AmpliSeq detected *KRAS* mutations in seven samples, while three samples remained negative (Supplementary Table S2). In addition to *KRAS*, the Bridge Capture 282-probe panel and the Ion AmpliSeq CHPv2 panel shared 33 other target genes. Among these, eight mutations were concordantly detected by both methods, including mutations in *TP53*, *APC*, and *PIK3CA* genes (Supplementary Table S2). The correlation between Bridge Capture and Ion AmpliSeq VAF values for all oncogenic mutations was strong, with a r_s of 0.74 (95% CI: 0.35–0.91; $P<0.0024$) (Fig. 2b).

Cross-validation of the discrepant results between Bridge Capture and ddPCR

Of the 80 plasma samples analyzed by Bridge Capture and ddPCR, 12 showed discrepant results necessitating cross-validation with other methods. For that we utilized the Idylla ct*KRAS* Mutation Assay results and performed an additional analysis with Ion AmpliSeq CHPv2. Of the eight samples that were positive by Bridge Capture but negative by ddPCR, three were also reported positive by Idylla (among the five successfully analyzed), and one

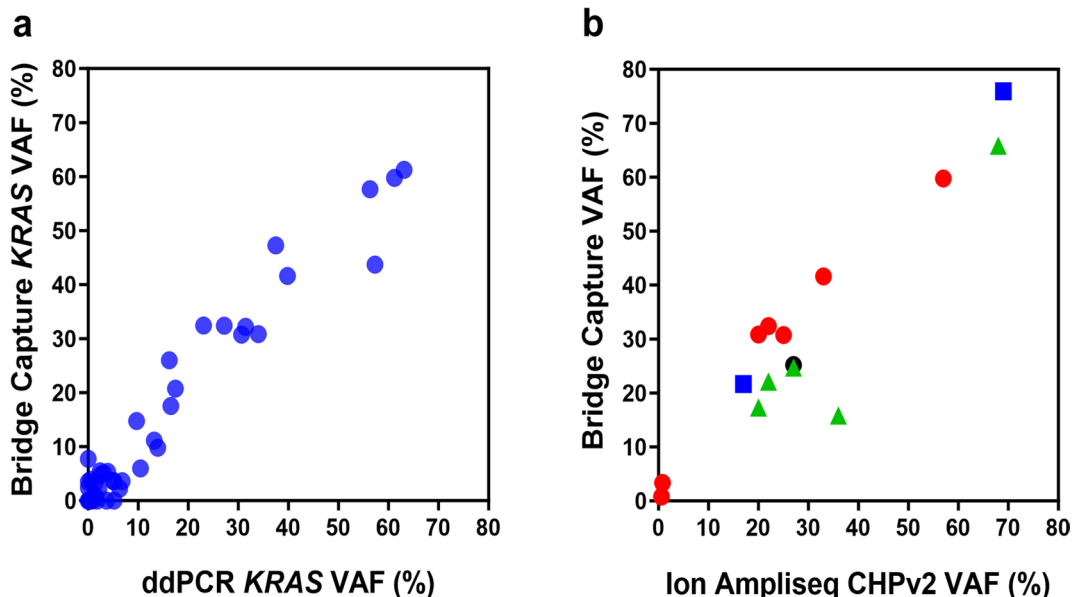


Fig. 2. Correlation of VAF values between Bridge Capture and the reference platform in ctDNA derived from plasma samples of mCRC patients. **(a)** Bridge Capture compared to ddPCR in detecting *KRAS* mutations (blue circles) in 80 ctDNA samples. The Spearman correlation coefficient (r_s) was 0.86. **(b)** Bridge Capture compared to Ion AmpliSeq CHPv2 in detecting oncogenic mutations, i.e. *KRAS* (red circles), *TP53* (green triangles), *APC* (blue squares), and *PIK3CA* (black circle) mutations in ten mCRC ctDNA samples. r_s was 0.74.

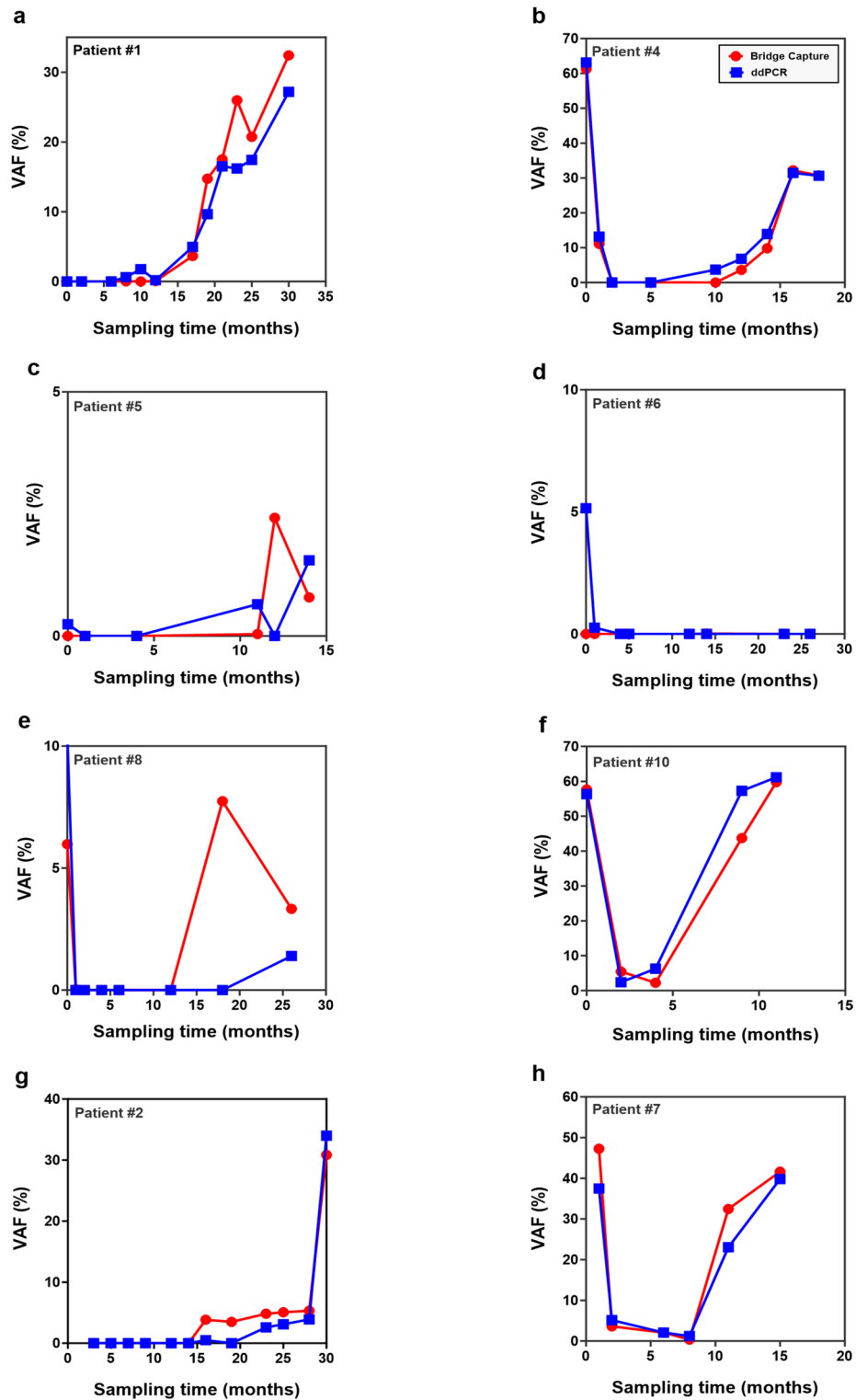


Fig. 3. KRAS VAF values detected in ctDNA derived from serial plasma samples of mCRC patients and analyzed using Bridge Capture (red circles) and ddPCR (blue squares). The patients in (g) and (h) lacked the baseline sample. Patient #6 (d) was the only long-term survivor, while all other patients deceased within approximately six months after the last plasma sample.

of these was additionally positive with the Ion AmpliSeq panel (Table 2). At least one sample was thus suggested to be a true positive result. In the subset of four samples that were negative by Bridge Capture but positive by ddPCR, three were reported positive by Idylla (one being invalid), and two of them were additionally positive with the Ion AmpliSeq. These results thus seem to be false negatives in the Bridge Capture analysis.

		Bridge Capture	
		Positive	Negative (VAF 0%)
Idylla	Positive	31	4
	Negative	2	21

Table 3. Concordance between Bridge Capture and Idylla ctKRAS mutation assay in detecting KRAS mutations in ctDNA samples ($n=58$). Cohen's Kappa-value was 0.79.

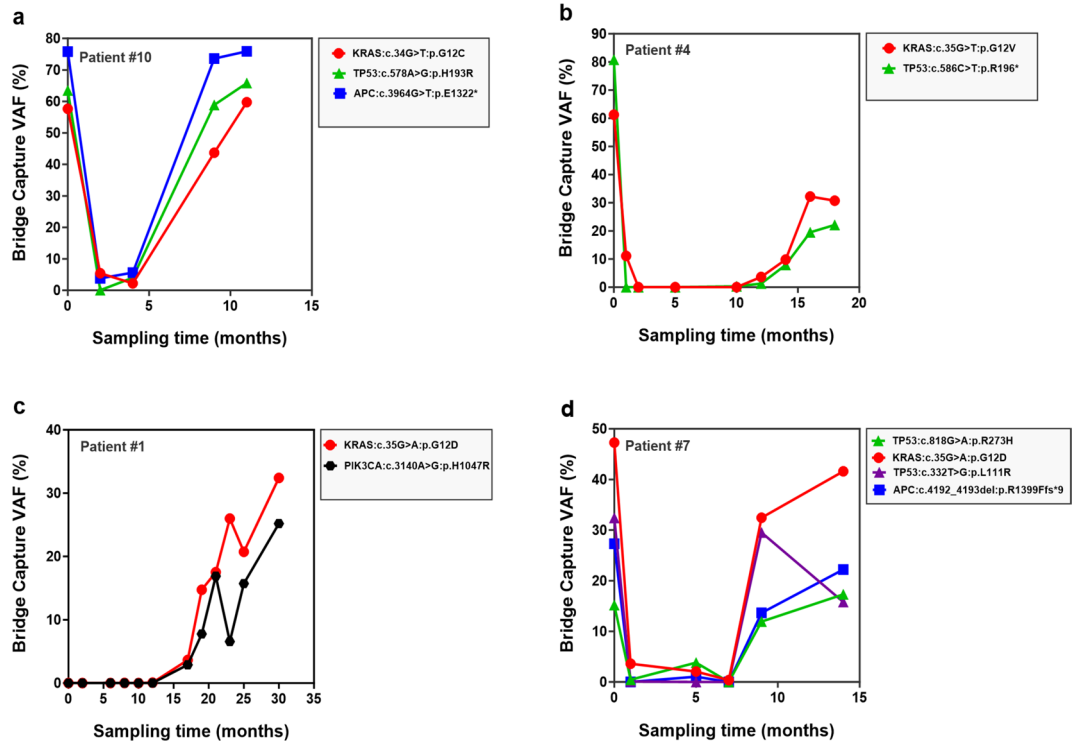


Fig. 4. Bridge Capture detected several oncogenic mutations in KRAS (red circles), TP53 (green triangles, purple triangles), APC (blue squares), and PIK3CA (black hexagons) genes as analyzed in ctDNA derived from serial plasma samples of mCRC patients.

Bridge Capture identified several oncogenic mutations in the ctDNA samples

Bridge Capture detected several DNA variants in addition to those found in the KRAS gene. Among the somatic mutations classified by COSMIC, variants recurring in at least two plasma samples per patient were further analyzed using the OncoKB database (Supplementary Table S3). In patients #1, #4, #7 and #10, VAF values of one or more oncogenic TP53, APC, or PIK3CA mutations closely mirrored those of the KRAS mutations in the serial plasma samples (Fig. 4). Additionally, multiple oncogenic mutations were identified in both oncogenes and tumor suppressor genes, all exhibiting VAF values below 6% (Supplementary Table S3). Using OncoKB database, these variants were classified based on their oncogenicity into the following categories: oncogenic, gain-of-function (e.g. KRAS, PIK3CA); likely oncogenic, loss-of-function (e.g. CREBBP, TP53); likely oncogenic, likely loss-of-function (e.g. APC, BRCA2, CBL, FBXW7, PTEN, RB1, SMAD4, TP53, VHL); and likely oncogenic, likely gain-of-function (e.g. RAF1). Mutations in genes previously shown to be associated with clonal hematopoiesis (e.g. ASXL1, DNMT3A, KMT2D, SF3B1, and certain TP53 variants) were detected in the cfDNA of several patients^{17,18}.

Validation of an expanded Bridge Capture 851-panel using synthetic DNA targets

Design of the study involving the analytical performance and scalability of Bridge Capture using synthetic DNA targets and an expanded 851-probe panel is shown in Fig. 1b. A dilution series of synthetic target pools mimicking VAF values between 0.0078% and 1% for all 851 probe targets was used. As shown in Fig. 5a, the dilutions from 0.0313 to 1% displayed a very strong linear correlation between the observed and expected total specific VAF signals for all probes (Pearson r and R^2 were 0.99 and 0.97, respectively). The two lowest VAF values (0.0078% and 0.0156%) were detected by Bridge Capture, but they did not fit to the linear regression model. This may imply that the system is at its lowest detection limit, influenced by stochastic effect and leading to variability in the detection. Another possibility is a contamination. The distribution of the r and R^2 values of

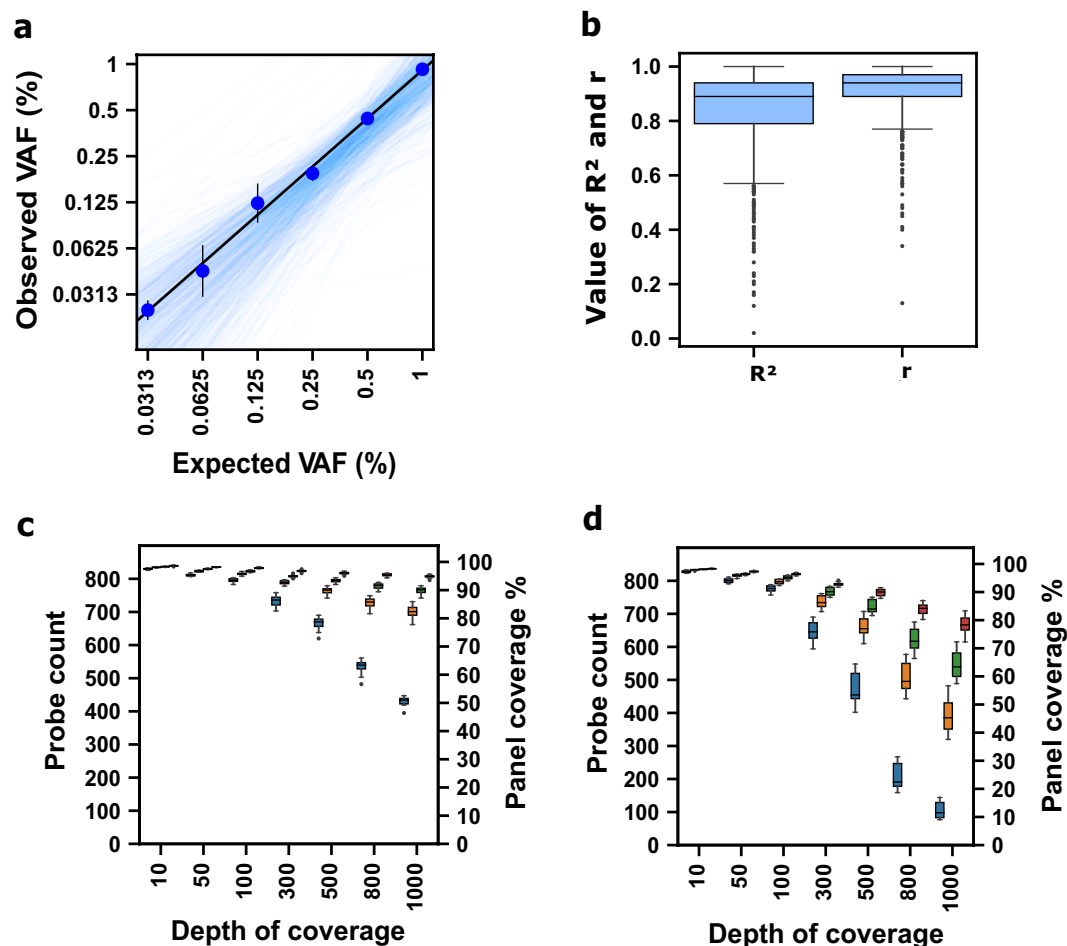


Fig. 5. Validation of an expanded Bridge Capture 851-probe panel using synthetic DNA targets. **(a)** Correlation between the observed specific VAF values and the expected VAF values. Blue circles represent the total specific VAF values for all probes shown as means \pm SD of five replicates, and black line represents their linear regression. Linear regressions of individual probes are shown with thin blue lines. **(b)** Box plots representing the distribution of r and R^2 values of individual probes. **(c)** Panel uniformity for read depth coverage across sequencing depths 15.8 M (red), 5 M (green), 2.5 M (orange), and 1 M (blue) paired-end reads. **(d)** Panel uniformity for unique read depth coverage at the same sequencing depths.

individual probes between VAF values 0.0313% and 1% is displayed in Fig. 5b. The median value of r was 0.94 (IQR 0.89–0.97) and that of R^2 was 0.89 (IQR 0.79–0.94).

To evaluate panel uniformity, the obtained sequencing reads were subsampled to varying sequencing depths, and the percentages of probes achieving 10x, 50x, 100x, 300x, 500x, 800x, and 1000x read depth coverage were calculated for each depth. At sequencing depths 15.8 M, 5 M, 2.5 M, and 1 M paired-end reads, the percentage of probes reaching 1000x total read depth coverage were 95%, 90%, 82%, and 51%, respectively (Fig. 5c). The values for unique reads were 78%, 63%, 45%, and 12% (Fig. 5d). Across all tested sequencing depths, over 90% of the targets reached 100x coverage ranging from 98 to 94% for total reads and from 96 to 91% for unique reads.

To further assess probe reproducibility, ten replicates of pool 1 consisting of wild-type targets were analyzed. Between the replicates, relative variation to the mean probe signal fell within 2-fold, 1-fold, and half-fold range for 99%, 90%, and 61% of the probes in the panel, respectively (Supplementary Fig. S2). Only eight (1%) of the 851 probes showed larger than 2-fold variation.

Discussion

This study demonstrates the utility of the novel NGS-based Bridge Capture technology for mutation profiling in liquid biopsies from mCRC patients, comparing its performance to those of ddPCR, Ion AmpliSeq, and Idylla. Bridge Capture showed a strong correlation with other technologies in VAF values and a substantial agreement in concordance. Discrepancies between the methods were primarily observed at low VAF values and/or low cfDNA input.

In clinical practice, ddPCR is widely used due to its high sensitivity and specificity for detecting low-frequency mutations, with the detection limit being as low as VAF value 0.01% for ctDNA⁹. However, ddPCR has a limited use for tumor-agnostic disease monitoring, as it can detect only a few predefined targets per assay¹⁹. The Bridge

Capture platform showed substantial agreement and very strong correlation with ddPCR in detecting *KRAS* mutations. The discrepancy between Bridge Capture and ddPCR in detecting certain low VAF *KRAS* mutations may be attributed to the input quantity of cfDNA. Notably, samples that were discrepant between Bridge Capture and ddPCR had a lower cfDNA input than those that were positive with both methods. Supporting this, other studies have shown that reducing cfDNA input from 25 ng to 10 ng significantly decreases sensitivity and reproducibility in NGS-based ctDNA assays²⁰. One of the key advantages of Bridge Capture technology is its ability to utilize a relatively large sample volume and cfDNA input, contributing to increased sensitivity. This may partly explain the eight samples that tested positive with Bridge Capture but were negative by ddPCR, among which Idylla identified three as positive, and Ion AmpliSeq confirmed one. On the other hand, two samples that were negative by Bridge Capture but positive by ddPCR were confirmed as potential false negatives in the Bridge Capture analysis.

A subset of the Bridge Capture and ddPCR concordant ctDNA samples were also analyzed by Ion AmpliSeq CHPv2. Across 33 shared target genes, both methods detected 15 mutations in *KRAS*, *TP53*, *APC*, and *PIK3CA* genes. Bridge Capture also identified several additional mutations, showcasing its broad mutation profiling capability. In addition to the known *KRAS* mutations, Bridge Capture identified several other CRC driver mutations mirroring the VAF values of *KRAS* in the serial plasma samples. This demonstrates the potential of Bridge Capture to be used in a tumor-agnostic manner, i.e. without knowledge of the mutation profile of the tumor, in disease monitoring.

Further, Bridge Capture detected several other oncogenic mutations, especially at low VAF values. Part of these mutations may derive from clonal hematopoiesis, especially in older patients^{17,18}. However, some of the identified mutations have been reported to be driver mutations of CRC, including *CREBBP*, *SMAD4*, *RB1*, and *RAF1*²¹. These findings confirm that Bridge Capture provides reliable mutation detection and could be used for MRD monitoring, with the advantage of higher multiplexing capabilities.

To validate the analytical performance and scalability of the technology, we used synthetic DNA targets providing a range of VAF values for each probe. The observed and expected VAF values showed a very strong linear correlation down to 0.03%. The probes within the 851-probe panel displayed minimal signal variation providing reproducible detection between the replicates. We demonstrated that panel evenness remained high across different depths of coverage for both total and unique reads. At as low as 1 M sequencing depth, 100 probes reached 1000x unique coverage. At sequencing depths of 2.5 M and 5 M, 380 and 540 probes were able to reach 1000x unique coverage, respectively. These results highlight that even at moderate sequencing depths, a large proportion of the panel achieves high coverage. Lower sequencing depth enables the analysis of larger number of samples within one sequencing run, leading to decreased cost per sample²². The results obtained with synthetic targets are indicative, since natural DNA is more complex and heterogeneous. Nevertheless, the synthetic templates provide valuable information about the performance and detection capabilities of each probe in the panel, which is not possible with native DNA.

The main shortcoming of the study is a relatively limited sample material that consisted of exclusively mCRC patients. The ctDNA detection rate in CRC is among the highest in patients with advanced cancers²³. Therefore, this study does not show whether Bridge Capture performs equally well in ctDNA analysis of other malignant diseases. Another limitation is the strong focus on *KRAS* mutations. Future studies of Bridge Capture technology should include validation in larger and more diverse clinical cohorts and other cancer types to prove its universal applicability in monitoring treatment response and disease progression.

In conclusion, this study demonstrates for the first time the potential of Bridge Capture as a promising technology for mutation profiling in plasma samples from mCRC patients. Bridge Capture shows substantial concordance with other technologies in clinical sample validation, with VAF values strongly correlating with those from ddPCR and the NGS-based Ion AmpliSeq analyses, underscoring its reliability. Additionally, the probe panel demonstrates high scalability, as shown by experiments with synthetic DNA. Furthermore, this study highlights the capability of Bridge Capture to reliably detect treatment-guiding mutations through a multiplexed approach. Validating these findings in larger, more diverse cohorts will be crucial for their translation into clinical practice.

Methods

Patient cohort, collection of plasma samples, and extraction of cfDNA

All mCRC patient samples were derived from a cohort of 77 participants enrolled in the AXOAXI phase II trial conducted at the Helsinki University Hospital between April 2015 and March 2017 (NCT01531595; EudraCT 2011-003137-33)²⁴. Ten patients who were identified to have a *KRAS* codon 12 or 13 mutation (G12D, G12V, G12C, G13D, or G13R) in their primary tumor resection specimen were included in this study. Blood samples were collected at multiple time points, i.e. prior to treatment initiation (baseline for 6/10 patients), after the first treatment cycle (three weeks), at each treatment response evaluation (every nine weeks), during first-line therapy, and at disease progression during subsequent treatment lines. Between 5 and 12 samples were retrieved from each patient, resulting in a total of 80 blood samples. The samples were collected in EDTA tubes and centrifuged within 30 min to separate plasma. Plasma was immediately stored at -20°C and transferred to -80°C within two weeks. cfDNA was extracted from 2 mL of plasma with automated QIA Symphony SP instrument using the QIA Symphony DSP Circulating DNA Kit (Qiagen, Hilden, Germany) and elution volume of 60 μL . After extraction, the cfDNA samples were stored at -80°C . The same cfDNA eluate was used for analysis with Bridge Capture, ddPCR, and Ion AmpliSeq, which were performed at different time points. cfDNA concentration was measured using the Qubit[™] dsDNA HS Assay Kit and Qubit[™] 4.0 Fluorometer (Thermo Fisher Scientific, Waltham, MA, USA). Across all measurable serial plasma samples, median cfDNA concentration was 0.45 ng/ μL (range 0.05–22.7 ng/ μL ; Supplementary Table S1). Written informed consent was obtained from all patients, and the study was performed in accordance with the relevant guidelines and regulations, including the Declaration

of Helsinki. The study protocol was approved by the Ethical Review Board of Helsinki University Hospital. Patient characteristics have been described earlier in Holm et al.¹⁵.

Synthetic DNA targets

Two pools of synthetic targets, each containing 887 templates¹⁴ were produced by Twist Bioscience (South San Francisco, CA, USA). Pool 1 consisted of the wild-type target sequences for Bridge Capture™ probe panel (Supplementary Table S4). Pool 2 contained templates identical to those in Pool 1, except for three centermost nucleotides, which were complemented. The pools were dissolved in nuclease free water to achieve a concentration of 10⁵ copies/μL for each individual template. The wild-type and altered pools were then mixed in varying ratios to mimic allelic fractions of 1%, 0.5%, 0.25%, 0.125%, 0.0625%, 0.0313%, 0.0156%, and 0.0078%. Each serial dilution was tested in five replicates. The blank sample (pool 1) was tested in ten replicates.

Bridge Capture™

The cfDNA samples ($n=80$) and synthetic DNA targets were analyzed using the Bridge Capture platform, which is based on a proprietary Bridge Capture technology from Genomill Health Inc, Turku, Finland¹⁴. For the analysis of patient samples, 35 μL of cfDNA was used, and the samples underwent an overnight target capture with a 282-probe panel covering 84 genes (Supplementary Table S5). For the synthetic DNA templates, 10 μL of mixed synthetic sample was used as an input, and the samples were incubated overnight with an 851-probe panel covering 121 genes (Supplementary Table S4). The indexed libraries were purified with Agencourt Ampure XP beads (Beckman Coulter, Brea, CA, USA) and quantified using a Qubit™ 4.0 Fluorometer. Sequencing was performed on a NovaSeq 6000 system using NovaSeq 6000 SP Reagent Kit v1.5 (300 cycles) and paired-end reads (Illumina, San Diego, CA, USA).

Bridge Capture data analysis

With Bridge Capture, the mean raw sequencing depth for ctDNA samples was 2.76 million reads per sample, with a median of 70% on-target reads (raw reads aligning to correct loci). Minimum depth of coverage for the probe targeting *KRAS* codons 12 and 13 was 1485 reads after UMI-based error correction. For synthetic DNA targets, the mean raw sequencing depth was 16.5 million reads per sample, with a median of 94% on-target reads. For the data analysis, the paired-end reads were merged using VSEARCH18 (v2.15.2_linux_x86_64) with the following parameters: `--fastq_minovlen 10 --fastq_maxdiffs 15 --fastq_maxee 1 --fastq_allowmergestagger`. A proprietary pipeline utilizing UMI-based error-correction was used to process the merged reads, and VAF values were calculated using read counts. Specific VAF values for the synthetic DNA targets were obtained by subtracting the mean signal of blank samples (wild-type targets only). Two replicates, one from the 0.0313% sample and one from the 0.0625% sample, were excluded from the linear regression analysis because their VAF values exceeded the upper bound of the interquartile range ($Q3 + 1.5 \times IQR$). Supplementary Table S6 shows the expected and observed total VAF values (%) for all replicates, with outlier status indicated. For figures of synthetic DNA target validation, Python (v3.11.5) was utilized with the matplotlib (v3.7.2) library. All other figures were made using Prism 10 (v10.1.2; GraphPad Software, San Diego, CA, USA).

Droplet digital PCR

The cfDNA samples ($n=80$) were analyzed using ddPCR with validated mutation detection assays for *KRAS*, including mutations G12D (Assay ID: dHsaCP2000001), G12V (dHsaCP2000005), G12C (dHsaCP2000007), G13D (dHsaCP25005989), and G13R (dHsaCP2506874) (all from Bio-Rad, Hercules, CA, USA). For the assay, 2 μL of cfDNA was added into a 20 μL PCR reaction (final volume), which was partitioned into 20,000 droplets using the Bio-Rad QX200 Droplet Generator. The samples were analyzed in duplicates. Following amplification, positive and negative droplets were detected with Bio-Rad QX200 Droplet Reader. The results were analyzed with QuantaSoft Analysis Pro Software (v.1.0, Bio-Rad), and a sample was considered positive if at least one positive droplet (Mut/Mut) was detected in both duplicate reactions. The final mutation frequency was calculated as the total number of mutant-positive droplets (Mut/Mut and Mut/Wt) divided by the total number of all droplets.

Ion AmpliSeq™ Cancer Hotspot Panel v2

Two μL of cfDNA derived from the last serial plasma sample of each patient ($n=10$) was analyzed using the Ion AmpliSeq Cancer Hotspot Panel v2 (Thermo Fisher Scientific) according to manufacturer's instructions. This panel covers the hotspot regions in 50 oncogenes and tumor suppressor genes (Supplementary Table S7). Obtained libraries were pooled, loaded onto the Ion PI™ Chip using the Ion Chef™ instrument, and sequenced with the Ion Proton™ System (Thermo Fisher Scientific). The detection limit used was 2% VAF at a sequencing coverage depth from 1000x to 2500x or 0.5% VAF at coverage depth over 2500x. Additionally, the 12 discrepant samples between ddPCR and Bridge Capture were validated with Ion AmpliSeq.

Idylla™ ctKRAS mutation assay

Of the cfDNA sample set ($n=80$), 65 plasma samples were analyzable using the fully automated real-time PCR-based Idylla ctKRAS Mutation Assay (Biocartis, Mechelen, Belgium). The analysis was performed according to the manufacturer's instructions, with 1 mL of plasma loaded into the cartridge along with 50 μL of proteinase K enzyme. This assay detects 21 different *KRAS* mutations in exons 2, 3, and 4 (Supplementary Table S8).

Categorization of the identified mutations

All additional mutations identified by Bridge Capture were analyzed using the Catalogue of Somatic Mutations in Cancer (COSMIC; v101; <https://cancer.sanger.ac.uk/cosmic>)²⁵ and classified into Tier 1 (strong evidence of oncogenicity; pathogenic), Tier 2 (moderate evidence; likely pathogenic), and Tier 3 (limited or uncertain

evidence). Germline variants were interpreted using ClinVar (<https://www.ncbi.nlm.nih.gov/clinvar/>)²⁶. Among the somatic mutations classified by COSMIC, variants recurring in at least two plasma samples per patient were further analyzed using the OncoKB (<https://www.oncokb.org/>)^{27,28}. Based on OncoKB, the variants were annotated into the following categories: oncogenic, gain-of-function; oncogenic, loss-of-function; likely oncogenic, loss-of-function; likely oncogenic, likely loss-of-function; likely oncogenic, likely gain-of-function; likely oncogenic, switch-of-function; and inconclusive.

Statistical analysis

The degree of agreement between Bridge Capture and ddPCR or Idylla was quantified using the kappa statistic (GraphPad Quick-Calcs; <https://www.graphpad.com/quickcalcs/kappa1/>). All other statistical analyses of ctDNA samples, including calculations of r_s , were performed using Prism 10 (v10.1.2). The Spearman r_s was used due to the non-normal distribution of KRAS VAF values, as assessed by the Kolmogorov-Smirnov and Shapiro-Wilk tests. Statistical analyses of synthetic DNA target validation were performed with Python (v3.11.5). The R^2 scores were calculated using sklearn library (v1.2.2), while linear regressions were performed using the scipy library (v1.11.1). P -values below 0.05 were considered statistically significant.

Data availability

The original contributions presented are included in the article or Supplementary Material. The raw sequencing data of patient cfDNA samples cannot be publicly available due to privacy protection regulations. However, they are available from the corresponding authors upon request. All sequence data generated in the validation assay using synthetic DNA targets, have been deposited in the Sequence Read Archive (SRA) at NCBI and made publicly available at <http://www.ncbi.nlm.nih.gov/bioproject/1267295>, with accession number PRJNA1267295.

Received: 21 March 2025; Accepted: 29 May 2025

Published online: 01 July 2025

References

- Bray, F. et al. Global cancer statistics 2022: GLOBOCAN estimates of incidence and mortality worldwide for 36 cancers in 185 countries. *CA Cancer J. Clin.* **74**, 229–263. <https://doi.org/10.3322/caac.21834> (2024).
- Cervantes, A. et al. Metastatic colorectal cancer: ESMO clinical practice guideline for diagnosis, treatment and follow-up. *Ann. Oncol.* **34**, 10–32. <https://doi.org/10.1016/j.annonc.2022.10.003> (2023).
- Saoudi Gonzalez, N. et al. Unravelling the complexity of colorectal cancer: heterogeneity, clonal evolution, and clinical implications. *Cancers (Basel)*. **15**, 4020. <https://doi.org/10.3390/cancers15164020> (2023).
- Kiran, N. S., Yashaswini, C., Maheshwari, R., Bhattacharya, S. & Prajapati, B. G. Advances in precision medicine approaches for colorectal cancer: from molecular profiling to targeted therapies. *ACS Pharmacol. Transl. Sci.* **7**, 967–990. <https://doi.org/10.1021/acscptsci.4c00008> (2024).
- László, L. et al. Recent updates on the significance of KRAS mutations in colorectal cancer biology. *Cells* **10**, 667. <https://doi.org/10.3390/cells10030667> (2021).
- Malla, M., Loree, J. M., Kasi, P. M. & Parikh, A. R. Using circulating tumor DNA in colorectal cancer: current and evolving practices. *J. Clin. Oncol.* **40**, 2846–2857. <https://doi.org/10.1200/JCO.21.02615> (2022).
- Tao, X. Y., Li, Q. Q. & Zeng, Y. Clinical application of liquid biopsy in colorectal cancer: detection, prediction, and treatment monitoring. *Mol. Cancer*. **23**, 145. <https://doi.org/10.1186/s12943-024-02063-2> (2024).
- Li, D. et al. Standardization of the liquid biopsy for pediatric diffuse midline glioma using ddPCR. *Sci. Rep.* **11**, 5098. <https://doi.org/10.1038/s41598-021-84513-1> (2021).
- Palacin-Aliana, I. et al. Clinical utility of liquid biopsy-based actionable mutations detected via ddPCR. *Biomedicines* **9**, 906. <https://doi.org/10.3390/biomedicines9080906> (2021).
- Uguen, A. & Troncone, G. A review on the Idylla platform: towards the assessment of actionable genomic alterations in one day. *J. Clin. Pathol.* **71**, 757–762. <https://doi.org/10.1136/jclinpath-2018-205189> (2018).
- Rachiglio, A. M. et al. Dynamics of RAS/BRAF mutations in cfDNA from metastatic colorectal carcinoma patients treated with polychemotherapy and anti-EGFR monoclonal antibodies. *Cancers (Basel)*. **14**, 1052. <https://doi.org/10.3390/cancers14041052> (2022).
- Bayle, A. et al. Circulating tumor DNA landscape and prognostic impact of acquired resistance to targeted therapies in cancer patients: a national center for precision medicine (PRISM) study. *Mol. Cancer*. **22**, 176. <https://doi.org/10.1186/s12943-023-01878-9> (2023).
- Wang, W. et al. Plasma ctDNA enhances the tissue-based detection of oncogene mutations in colorectal cancer. *Clin. Transl. Oncol.* **26**, 1976–1987. <https://doi.org/10.1007/s12094-024-03422-7> (2024).
- Adamusová, S. et al. Bridge Capture permits cost-efficient, rapid and sensitive molecular precision diagnostics. *MedRxiv*. <https://doi.org/10.1101/2024.04.12.24301526> (2025).
- Holm, M. et al. Detection of KRAS mutations in liquid biopsies from metastatic colorectal cancer patients using droplet digital PCR, Idylla, and next generation sequencing. *PLoS One*. **15**, e0239819. <https://doi.org/10.1371/journal.pone.0239819> (2020).
- Bando, H. et al. Effects of metastatic sites on circulating tumor DNA in patients with metastatic colorectal cancer. *JCO Precis Oncol.* **6**, e2100535. <https://doi.org/10.1200/PO.21.00535> (2022).
- Razavi, P. et al. High-intensity sequencing reveals the sources of plasma circulating cell-free DNA variants. *Nat. Med.* **25**, 1928–1937. <https://doi.org/10.1038/s41591-019-0652-7> (2019).
- Arends, C. M. et al. Dynamics of clonal hematopoiesis under DNA-damaging treatment in patients with ovarian cancer. *Leukemia* **38**, 1378–1389. <https://doi.org/10.1038/s41375-024-02253-3> (2024).
- Decraene, C. et al. Multiple hotspot mutations scanning by single droplet digital PCR. *Clin. Chem.* **64**, 317–328. <https://doi.org/10.1373/clinchem.2017.272518> (2018).
- Harter, J. et al. Analytical performance evaluation of a 523-gene circulating tumor DNA assay for next-generation sequencing-based comprehensive tumor profiling in liquid biopsy samples. *J. Mol. Diagn.* **26**, 61–72. <https://doi.org/10.1016/j.jmoldx.2023.10.001> (2024).
- Cornish, A. J. et al. The genomic landscape of 2,023 colorectal cancers. *Nature* **633**, 127–136. <https://doi.org/10.1038/s41586-024-07747-9> (2024).
- Meldrum, C., Doyle, M. A. & Tothill, R. W. Next-generation sequencing for cancer diagnostics: a practical perspective. *Clin. Biochem. Rev.* **32**, 177–195 (2011).

23. Odegaard, J. I. et al. Validation of a plasma-based comprehensive cancer genotyping assay utilizing orthogonal tissue- and plasma-based methodologies. *Clin. Cancer Res.* **24**, 3539–3549. <https://doi.org/10.1158/1078-0432.CCR-17-3831> (2018).
24. Osterlund, P. et al. SO-18 Single-arm multicentre phase II study of bevacizumab (B) combined with 9-weekly alternating CAPOX and CAPIRI as first-line treatment of patients with metastatic colorectal cancer (mCRC): main results of the AXOAXI-trial. *Ann. Oncol.* **31**. <https://doi.org/10.1016/j.annonc.2020.04.033> (2020).
25. Tate, J. G. et al. COSMIC: The Catalogue of Somatic Mutations in Cancer. *Nucleic Acids Res.* **47**, D941–D947. <https://doi.org/10.1093/nar/gky1015> (2019).
26. Landrum, M. J. et al. ClinVar: public archive of relationships among sequence variation and human phenotype. *Nucleic Acids Res.* **42**, D980–D985. <https://doi.org/10.1093/nar/gkt1113> (2014).
27. Chakravarty, D. et al. OncoKB: a precision oncology knowledge base. *JCO Precis Oncol.* **1**, 1–16. <https://doi.org/10.1200/PO.17.0011> (2017).
28. Suehnholz, S. P. et al. Quantifying the expanding landscape of clinical actionability for patients with cancer. *Cancer Discov.* **14**, 49–65. <https://doi.org/10.1158/2159-8290.CD-23-0467> (2024).

Acknowledgements

The authors thank Merja Haukka and Hanna Tammio for excellent technical assistance.

Author contributions

Conceptualization and design: AK, SA, PO, JPP, MT, and AR. Data curation: AG, AK, AM, TR, NL, EO, JK, SK, PO, and AR. Formal analysis: AG, AK, PN, and AR. Funding acquisition: JB, PO, MT, and AR. Investigation: AG, AK, SA, AM, TR, NL, EA, EO, AO, PH, TH, and PO. Methodology: AK, SA, AM, TR, NL, EA, AO, TH, SK, JPP, and MT. Project administration: SK, JPP, MT, and AR. Resources: AKA, PO, MT, and AR. Supervision: JL, SK, JPP, PN, MT, and AR. Software: AK, NL, SK, and MT. Validation: AG, AK, AS, HM, and SK. Visualization: AG, AK, PN, and AR. Writing – original draft: AG, AK, and SA. Writing – review & editing: all authors.

Funding

This study was supported by Almaral, Avohoidon Tutkimussäätiö, the Cancer Foundation Finland, Finska Läkaresällskapet, Helsinki University Hospital Research Funds, iCANDOC National Doctoral Education Pilot in Precision Cancer Medicine, Medicinska Understödsföreningen Liv och Hälsa, the Sigrid Jusélius Foundation, the University of Helsinki, and Voima Ventures. The funding sources had no role in study design, data collection and analysis, decision to publish, or preparation of the manuscript.

Declarations

Competing interests

MT is a Chief Technology Officer and Interim CEO of Genomill Health Inc. JL is a medical advisor to Genomill. JL, JB, and MT hold equity in Genomill. AK, SA, AM, TR, NL, TH, JK, JL, JB, JPP, and MT are entitled to stock options in Genomill. The authors AK, SA, AM, TR, NL, TH, JK and JPP are currently employed at Genomill. The research detailed in this manuscript is related to Genomill patents EP-3673081, JP-7074978, EP-4060049, US-11486003 and EP-4060050. Genomill is in the process of filing patents related to this work, and AK, TH, JPP, and MT and are named inventors on these patent applications. The other authors have no competing interests.

Additional information

Supplementary Information The online version contains supplementary material available at <https://doi.org/10.1038/s41598-025-04827-2>.

Correspondence and requests for materials should be addressed to A.G. or M.T.

Reprints and permissions information is available at www.nature.com/reprints.

Publisher's note Springer Nature remains neutral with regard to jurisdictional claims in published maps and institutional affiliations.

Open Access This article is licensed under a Creative Commons Attribution-NonCommercial-NoDerivatives 4.0 International License, which permits any non-commercial use, sharing, distribution and reproduction in any medium or format, as long as you give appropriate credit to the original author(s) and the source, provide a link to the Creative Commons licence, and indicate if you modified the licensed material. You do not have permission under this licence to share adapted material derived from this article or parts of it. The images or other third party material in this article are included in the article's Creative Commons licence, unless indicated otherwise in a credit line to the material. If material is not included in the article's Creative Commons licence and your intended use is not permitted by statutory regulation or exceeds the permitted use, you will need to obtain permission directly from the copyright holder. To view a copy of this licence, visit <http://creativecommons.org/licenses/by-nc-nd/4.0/>.

© The Author(s) 2025